Biochimica et Biophysica Acta 1847 (2015) 1220–1230

Contents lists available at ScienceDirect

Biochimica et Biophysica Acta

journal homepage: www.elsevier.com/locate/bbabio

Functional characterization and organ distribution of three mitochondrial ATP–Mg/P_i carriers in *Arabidopsis thaliana*

Magnus Monné [a,b], Daniela Valeria Miniero [a], Toshihiro Obata [c], Lucia Daddabbo [a], Luigi Palmieri [a], Angelo Vozza [a], M. Cristina Nicolardi [a], Alisdair R. Fernie [c], Ferdinando Palmieri [a,*]

[a] Department of Biosciences, Biotechnologies and Biopharmaceutics, University of Bari, Via E. Orabona 4, 70125 Bari, Italy
[b] Department of Sciences, University of Basilicata, Via Ateneo Lucano 10, 85100 Potenza, Italy
[c] Department Willmitzer, Max-Planck-Institut fur Molekulare Pflanzenphysiologie, Am Mühlenberg 1, 14476 Potsdam-Golm, Germany

ARTICLE INFO

Article history:
Received 16 April 2015
Received in revised form 15 June 2015
Accepted 29 June 2015
Available online 2 July 2015

Keywords:
Arabidopsis
ATP–Mg/phosphate carrier
Membrane transport
Mitochondria
Mitochondrial carrier
Mitochondrial transporter

ABSTRACT

The *Arabidopsis thaliana* genome contains 58 membrane proteins belonging to the mitochondrial carrier family. Three members of this family, here named *At*APC1, *At*APC2, and *At*APC3, exhibit high structural similarities to the human mitochondrial ATP–Mg^{2+}/phosphate carriers. Under normal physiological conditions the *AtAPC1* gene was expressed at least five times more than the other two *AtAPC* genes in flower, leaf, stem, root and seedlings. However, in stress conditions the expression levels of *AtAPC1* and *AtAPC3* change. Direct transport assays with recombinant and reconstituted AtAPC1, AtAPC2 and AtAPC3 showed that they transport phosphate, AMP, ADP, ATP, adenosine 5′-phosphosulfate and, to a lesser extent, other nucleotides. AtAPC2 and AtAPC3 also had the ability to transport sulfate and thiosulfate. All three AtAPCs catalyzed a counter-exchange transport that was saturable and inhibited by pyridoxal-5′-phosphate. The transport activities of AtAPCs were also inhibited by the addition of EDTA or EGTA and stimulated by the addition of Ca^{2+}. Given that phosphate and sulfate can be recycled via their own specific carriers, these findings indicate that AtAPCs can catalyze net transfer of adenine nucleotides across the inner mitochondrial membrane in exchange for phosphate (or sulfate), and that this transport is regulated both at the transcriptional level and by Ca^{2+}.

1. Introduction

Members of the mitochondrial carrier (MC) protein family transport nucleotides, amino acids, carboxylic acids, inorganic ions and cofactors across the mitochondrial inner membrane [1–4]. The transport steps catalyzed by MCs are important for connecting matrix and cytoplasmic pathways, e.g. for energy metabolism, gluconeogenesis, thermogenesis, fatty and amino acid metabolism, as well as for mitochondrial replication, transcription and translation. The protein sequences of MCs contain three tandemly repeated domains [5], of which each consists of about 100 residues including two hydrophobic segments and a signature sequence motif PX[D/E]XX[K/R]X[K/R] (20–30 residues) [D/E]GXXXX[W/Y/F][K/R]G (PROSITE PS50920, PFAM PF00153 and IPR00193) [6]. In the 3D-structures of carboxyatractyloside-inhibited ADP/ATP carriers the hydrophobic segments form a six-transmembrane α-helix bundle and the motifs PX[D/E]XX[K/R] participate in specific structural features that are proposed to be important for the transport mechanism [7–9]. The signature motif has been used to identify MCs in genomic sequences; 53 MCs are found in man, 35 in *Saccharomyces cerevisiae* and 58 in *Arabidopsis thaliana*; and for about half of these the substrates have been identified by direct transport assays [10,11].

The mitochondrial matrix is the site for oxidative phosphorylation where ATP synthase catalyzes the formation of ATP from ADP and phosphate (P_i) by using the electrochemical gradient generated by the respiratory chain complexes across the mitochondrial inner membrane. To export the product and import the substrates of ATP synthase, the produced matritial ATP is exchanged for cytosolic ADP by the mitochondrial ADP/ATP carrier, and P_i is imported into the matrix by the P_i carrier [12–16]. ADP/ATP carriers are strict antiporters and therefore do not catalyze any net transport of adenine nucleotides across the mitochondrial inner membrane, while the P_i carrier transports P_i unidirectionally. We recently identified ADNT1, a novel mitochondrial transporter in Arabidopsis which prefers AMP to ADP for counter-exchange with ATP and demonstrated that deficiency of this transporter lead to deficient respiration and root growth [17]. However, despite the clear importance of the above transporters, the regulation of some matrix adenine nucleotide-dependent processes requires that the intramitochondrial nucleotide pools change in a manner which can only be accomplished by a net import or export into or from the mitochondria. Such a

Abbreviations: APC, ATP–Mg/phosphate carrier; APS, adenosine 5′-phosphosulfate; AtAPC, *Arabidopsis thaliana*; ATP, Mg/phosphate carrier; MC, mitochondrial carrier; P_i, inorganic phosphate

* Corresponding author.
E-mail address: ferdpalmieri@gmail.com (F. Palmieri).

http://dx.doi.org/10.1016/j.bbabio.2015.06.015
0005-2728/

transport step is catalyzed by the ATP–Mg/P_i carrier (APC) that exchanges ATP for P_i, which is recycled back to the original compartment by the P_i carrier. The existence of a carboxyatractyloside-insensitive ATP/Pi exchanger was initially inferred from transport studies in isolated rat liver mitochondria ([18] and references therein). Three MCs responsible for the ATP–Mg/P_i transport were indeed identified in human by recombinant expression, reconstitution in liposomes and transport assays [19]. Apart from the typical MC sequences the APCs, as well as the aspartate/glutamate carriers [20], contain N-terminal EF-hand Ca^{2+}-binding domains that are important for transport regulation [19,21]. A few years later a fourth human ATP–Mg/P_i carrier (APC4), which is Ca^{2+}-independent, was identified in the human genome [22].

In *A. thaliana* three APCs have been predicted on the basis of sequence similarity [11], mitochondrial localization and ability to partly complement the growth defect of the yeast *Sal1* (APC) null mutant [23]. However, these three proteins have not been functionally characterized hitherto. In this study, we have determined the substrate specificities, kinetic parameters and Ca^{2+}-dependence of the three putative plant APCs as well as investigated their expression levels, organ and tissue distribution in Arabidopsis. The results indicate that these proteins are indeed APCs which likely play distinctive, yet important, physiological roles in regulating the mitochondrial adenine nucleotide pool particularly in stress conditions such as cold and to a lesser extent drought and salt stress in addition to in rapidly growing tissues such as developing embryos and pollen tissues and root cells.

2. Materials and methods

2.1. Sequence and structure analysis

The protein sequences of the human APC1 (NP_037518.3), APC2 (NP_077008.2) and APC3 (NP_443133.2) were used to screen the *Arabidopsis* genome in search for their closest homologues. In *A. thaliana* three sequences were clearly similar to the three human APCs, with >39% identical residues covering >89% of the sequence and a maximum E-value of $1e^{-99}$: At5g61810 (NP_568940) named AtAPC1, At5g51050 (NP_199918) named AtAPC2 and At5g07320 (NP_196349) named AtAPC3. The amino acid sequences were aligned with ClustalW. Homology models of the AtAPCs were built based on the structure of the bovine ADP/ATP transporter [7] for the C-terminal membrane domains and the structure of human APC1 [24] for the N-terminal Ca^{2+}-binding domains and evaluated as previously described [25].

2.2. Plant material and growth conditions

A. thaliana ecotype Columbia [Col-0] seeds were germinated on Murashige and Skoog plates (MS plate, [26]) containing 1% Suc in a growth chamber (100 μmol photons m^{-2} s^{-1}; 22 °C) under a long-day regime (16 h of light/8 h of dark) before transfer to soil in a climate-controlled chamber under the same photoperiod. Seedlings and other plant tissues were harvested for gene expression analyses at 10 days and 6 weeks after sawing respectively.

2.3. Promoter-β-glucuronidase (GUS) assay

Around 2 kbp regions of genomic DNA upstream of *Atapc1*, *Atapc2* and *Atapc3* genes were amplified by PCR with primers fused with Gateway *attB* sequence. The primer sequences are as follows; *Atapc1*, APC1PFR2: GGGGACAAGTTTGTACAAAAAAGCAGGCTCCACCactcagacatttctttggtttaggatcaga and APC1PRV: GGGGACCACTTTGTACAAGAAAGCTGGGTCtgctggttaacgatcaatcgagaaa; *Atapc2*, APC2PFR1: GGGGACAAGTTTGTACAAAAAAGCAGGCTCCACCattgattgttagggttttggtgatagattg and APC2PRV: GGGGACCACTTTGTACAAGAAAGCTGGGTCtttcgttggtaaaccaacatgagtcgt; for *Atapc3*, APC3PFR2: GGACAAGTTTGTACAAAAAAGCAGGCTCCACCttttcgtcttttatgcttgtttcttcattt and APC3RRV: GGGGACCACTTTGTACAAGAAAGCTGGGTCtgctgattcgcgatcaatatcga. The lower case represents the *attB* adapter sequences. The PCR products were cloned into pDONR207 vector by Gateway BP reaction (Life Technologies, CA) and then into pKGWFS7 vector by LR reaction. Resulted promoter-GUS constructs were used for *Agrobacterium* mediated Arabidopsis transformation by floral dip method [27]. The transgenic plants were selected on MS plates containing 50 μg ml^{-1} kanamycin and grown on soil to produce seeds. T1 seeds were used for the analysis. Whole seedlings and leaf, flower, silique and stem from adult plants were subjected to GUS activity staining as previously described [17]. Images were taken using a Leica MZ10F stereo microscope (Leica Microsystems, Wetzlar, Germany) equipped with a Leica digital camera DFC 420 C.

2.4. Expression analysis by real-time PCR

Total RNA from whole plants and roots of seedlings and leaves, stems and flowers of mature plants were harvested and snap frozen in liquid nitrogen for gene expression analysis. Total RNA was extracted from ground frozen materials by TRIzol reagent (Life Technologies). The reverse transcription was performed from 2 μg of total RNA by SuperScript III reverse transcriptase (Life Technologies) using oligo dT primer following DNase treatment by Turbo DNA free kit (Life Technologies). The primers for real time PCR were designed by QuantPrime as follows; for *Atpac1*, APC1qF: CGGAGCCAGGTCCTTTGATACAAC and APC1qR: TTTCAGAAACTCTTGGCCCATGC; *Atapc2*, APC2qF: AGCTCTTGGAGCAACCTGTGTC and APC2qR: GCTCGTTCCGCTTGCATTCTTG; *Atapc3*, APC3qF: CGAGATGGGCGTGTTGATTACC and APC3qR: AATGCCGGCCTTAACAAGAGC. Real time PCR using SYBR Green (Power SYBR Green, Applied Biosystems, Foster City, CA) was performed in an ABI PRISM 7900 HT (Applied Biosystems). The Arabidopsis S-adenosyl-L-methionine dependent methyltransferases gene (AT2G32170) was amplified in parallel as a reference gene [28]. The relative levels of gene expression were calculated as $2^{-\Delta Ct}$, where ΔCt sample is the C_t target gene − the C_t reference gene and Ct is the threshold cycle (i.e. the PCR cycle number at which emitted fluorescence exceeds 10 times the SD of baseline emissions).

2.5. Construction of expression plasmids for bacterial production

PCR using complementary sequence-based primers for each gene was used to amplify the coding sequences for AtAPC1 from a custom made synthetic gene (Invitrogen), and AtAPC2 and AtAPC3 from *Arabidopsis* flower cDNA. The forward and reverse oligonucleotide primers contained the restriction sites NdeI and HindIII (AtAPC1), BamI and HindIII (AtAPC2) or BamI and EcoRI (AtAPC3). The amplified gene fragments were cloned into the pMW7-vector and transformed in *Escherichia coli* TG1 cells (Invitrogen). Transformants were selected on LB (10 g/l tryptone, 5 g/l yeast extract, 5 g/l NaCl, pH 7.4) plates containing 100 μg/ml ampicillin. All constructs were verified by DNA sequencing.

2.6. Bacterial expression and purification

AtAPC1, AtAPC2 and AtAPC3 from *Arabidopsis* were overexpressed as inclusion bodies in the cytosol of *E. coli* as described previously, except that the host cells were Rosetta-gami B(DE3) (Novagen) [29,30]. Inclusion bodies were purified on a sucrose density gradient and were washed at 4 °C, first with TE buffer (10 mM Tris–HCl, 1 mM EDTA, pH 7.0), then once with a buffer containing 3% Triton X-114 (w/v), 1 mM EDTA, 10 mM PIPES pH 7.0 and 10 mM Na_2SO_4, and finally three times with TE buffer. The inclusion body proteins were solubilized in 1.8% sarkosyl (w/v) and diluted 1:10 with 10 mM PIPES pH 7.0, 0.6% Triton X-114 and 1.7 mg/ml cardiolipin (Sigma).

Unsolubilized material was removed by centrifugation (15,300 ×*g* for 10 min).

2.7. Reconstitution into liposomes

The solubilized recombinant proteins were reconstituted into liposomes [31–34]. The reconstitution mixture contained solubilized proteins (about 18 μg), 1% Triton X-114, 1.4% egg yolk phospholipids as sonicated liposomes, 20 mM substrate, 20 mM PIPES pH 7.0, 0.7 mg cardiolipin, and water to a final volume of 700 μl. These components were mixed thoroughly, and the mixture was recycled 13 times through a Bio-Beads SM-2 column (Bio-Rad).

2.8. Transport assays

External substrate was removed from proteoliposomes on a Sephadex G-75 columns pre-equilibrated with 10 mM PIPES and 50 mM NaCl pH 7.0. Transport at 25 °C was initiated by adding [^{14}C]ADP (Perkin Elmer) or [^{33}P]P_i (American Radiolabeled Chemicals Inc.) to substrate-loaded (exchange) or empty (uniport) proteoliposomes. Transport was terminated by adding 20 mM pyridoxal 5′-phosphate and 20 mM bathophenanthroline, which in combination inhibit the activity of several MCs completely and rapidly [35–39]. In controls, the inhibitors were added at the beginning together with the radioactive substrate according to the "inhibitor-stop" method [31]. Finally, the external substrate was removed and the radioactivity in the liposomes was measured. The experimental values were corrected by subtracting control values. The initial transport rates were calculated from the radioactivity incorporated into proteoliposomes in the initial linear range of substrate transport. For efflux measurements, proteoliposomes containing 5 mM internal ADP were loaded with 5 μM [^{14}C]ADP by carrier-mediated exchange equilibrium [40,41]. The external radioactivity was removed by passing the proteoliposomes through Sephadex G-75. Efflux was started by adding unlabeled external substrate or buffer alone, and terminated by adding the inhibitors indicated above.

2.9. Other methods

Proteins were analyzed by SDS-PAGE and stained with Coomassie Blue dye. The amount of purified AtAPC proteins was estimated by laser densitometry of stained samples using carbonic anhydrase as protein standard [42]. To assay the protein incorporated into liposomes, the vesicles were passed through a Sephadex G-75 column, centrifuged at 300,000 ×*g* for 30 min, and delipidated with organic solvents as previously described [43]. Then, the SDS-solubilized protein was determined by comparison with carbonic anhydrase in SDS gels. The share of protein incorporated into liposomes was about 16% of the protein added in the reconstitution mixture. The free Ca^{2+} concentration was measured by using Fura-2 (Invitrogen) according to the instructions of the manufacturer.

3. Results

3.1. Identification of AtAPC1, AtAPC2 and AtAPC3 of A. thaliana

The NCBI *A. thaliana* Protein BLAST was screened for homologues of the previously characterized human APCs [19]. The *Arabidopsis* proteins AtAPC1, AtAPC2 and AtAPC3 (encoded by At5g61810, At5g51050 and At5g07320, respectively) share the highest sequence identity with the human APCs and, as their human counterparts, contain Ca^{2+}-binding EF hands in their N-terminal domains [11,23]. APC2 is the closest human homologue of AtAPC1, AtAPC2 and AtAPC3 with 39%, 38% and 38% overall identical residues, respectively (Supplementary Table S1). The C-terminal domains of AtAPC1, AtAPC2 and AtAPC3 contain the typical tripartate structure and signature motifs of mitochondrial carriers (Supplementary Fig. S1); they share a higher ratio of identical residues with human APC2 (48%, 47% and 46%, respectively) compared to the N-terminal domain containing Ca^{2+}-binding EF hands (25%, 24% and 26%, respectively). The three *Arabidopsis* proteins share higher sequence identity between themselves with 67% to 81% overall identical residues, almost equally distributed between the N-terminal and the C-terminal domain.

The Ca^{2+}-binding EF hands of the three AtAPCs consist of the sequence DXDXDGXIXXXE of which the first aspartate is the most conserved residue. As all the EF hands of the human APCs, the EF hands of the AtAPCs belong to the EF-hand_7 family with the exception of the first EF hand of AtAPC2 that belongs to EF-hand_6 (Pfam PF13499, Supplementary Fig. S1 and Table S2). Both EF-hand_7 and EF-hand_6 belong to the pseudo-EF hands in which Ca^{2+}-binding involves backbone carbonyls apart from the side chains of aspartates and/or glutamates. In keeping with the characteristics of their human counterparts, the *Arabidopsis* proteins also have the specific sequence feature distinctive of the APC subfamily of MCs e.g. the lack of the first negatively charged residue of the third signature motif [11]. From structural homology models based on the X-ray structure of the bovine ADP/ATP carrier [7] it can be deduced that 73% of the residues lining the internal translocation cavity are identical (87% similar) in all six Arabidopsis and human APCs.

3.2. Gene expression analyses of the Atapc1, 2 and 3 genes

Organ and tissue specific expression of *Atapc* genes was analyzed by both promoter GUS assay and real time PCR. Activities of *Atapc2* and *Atapc3* promoters were slightly detected in flower petals and seedling leaves, respectively (Fig. 1, B–C). *Atapc1* promoter was much more active compared to the others especially in vascular tissues, in leaves of both seedlings and mature plants, stamen filaments and developing siliques (Fig. 1A). Given that GUS assays are not highly sensitive we additionally carried out quantitative RT-PCR measurements which revealed that *Atapc1* expressed more than five times than the other two genes in all organs (Fig. 2). *Atapc2* expressed more in aerial parts than roots and seedlings. *Atapc1* showed an expression pattern quite similar to *Atapc2* except for a higher expression level in flower than in the other tissues. *Atapc3* mRNA accumulated in seedlings ten times more than in the other organs (Fig. 2). Searching the Bioarray Resource (BAR; https://www.bar.utoronto.ca; [44]) of publically available microarray data allowed us to broaden this analysis to cover far more tissue types and experimental conditions. The compiled data for the three *Atapc* genes is provided in Supplementary Figs. S2 and S3. *Atapc1* is lowly expressed in roots and seeds while *Atapc3* is highly expressed in these tissues (Supplementary Fig. S2). Both genes are highly expressed in embryo, while *Atapc3* is highly expressed in the pollen. Expression of *Atapc2* is less variable among tissues than that of the other two genes (Supplementary Fig. S2). The *Atapc1* gene is strongly induced by cold stress both in roots and shoots (Supplementary Fig. S3). It is also induced by stresses causing dehydration, namely drought, salt and osmotic stresses, and to a lesser extent wounding. *Atapc2* and *Atapc3* genes are by contrast only slightly induced by cold and salt stresses and drought and wounding stresses, respectively (Supplementary Fig. S3). Similarly, using the ATTED II database [45] allowed us to identify genes exhibiting the most similar expression patterns as *Atapc* 1–3 (results being summarized in Supplementary Fig. S4 and Table S3). *Atapc2* is involved in a co-expressed network of genes induced under phosphate starvation including SPX domain genes, genes of glycerolipid metabolism and phosphatases (Supplementary Table S3). *Atapc3* is co-expressed with some genes involved in DNA replication and galacturonosyltransferases which may be related to starch and sucrose metabolism. While some genes are co-expressed with *Atpac1*, no common function could be found among them (Supplementary Table S3).

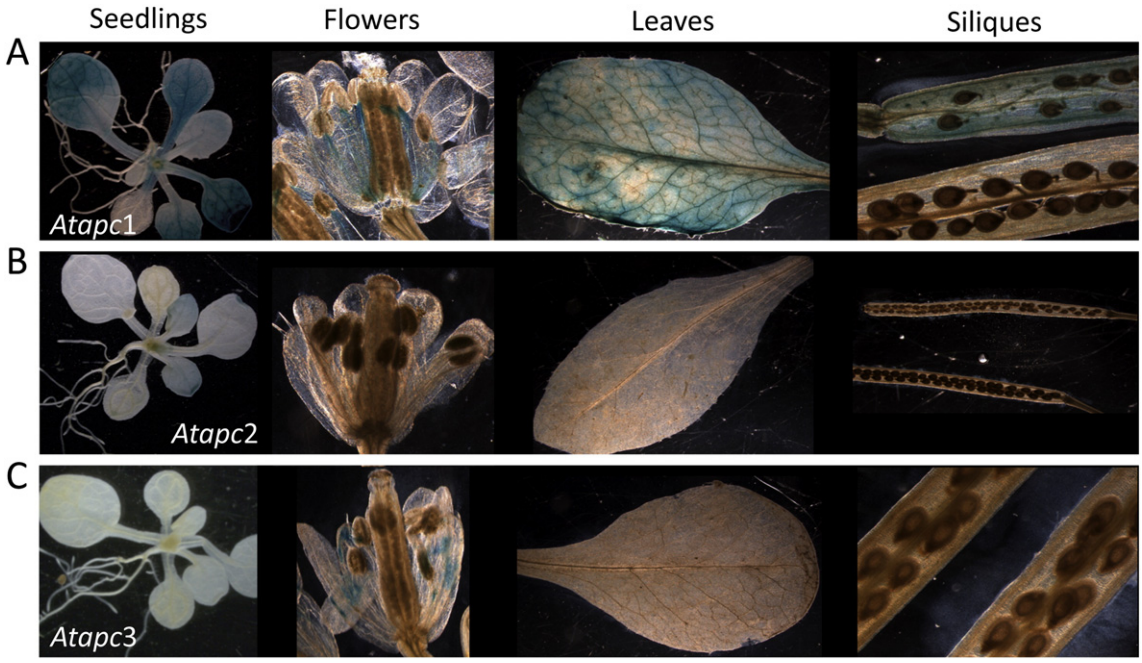

Fig. 1. GUS expression under control of the *Atapc1* (A), *Atapc2* (B) and *Atapc3* (C) promoters. Histochemical analysis of promoter activity in 10-day old seedlings and flowers, leaves and siliques of 6 week old plants.

3.3. Bacterial expression of AtAPCs

AtAPC1, AtAPC2 and AtAPC3 were expressed in *E. coli* Rosetta-gami B(DE3) strain (Fig. 3, lanes 4, 7 and 10). They accumulated as inclusion bodies and were purified by centrifugation and washing. The apparent molecular masses of purified AtAPC1, AtAPC2 and AtAPC3 (Fig. 3, lanes 5, 8 and 11) were approximately 53 kDa, which is in good agreement with the calculated values (53.3, 54.5 and 54.0 kDa for AtAPC1, AtAPC2 and AtAPC3, respectively). The yield of the purified proteins was about 40–60 mg/l of culture for all three AtAPCs. The proteins were not detected in un-induced cultures or in cultures with empty vector (Fig. 3, lanes 1, 3, 6 and 9).

3.4. Functional characterization of the recombinant AtAPCs

All three recombinant *Arabidopsis* proteins were reconstituted into liposomes, and their transport activities for ADP, ATP, AMP and P_i were tested in homo-exchange experiments, i.e. with the same substrate inside and outside the proteoliposomes. By using external and internal substrate concentrations of 1 and 20 mM, respectively, reconstituted AtAPC1, AtAPC2 and AtAPC3 all showed transport activity with these four substrates. These activities were completely inhibited by a mixture of pyridoxal-5′-phosphate and bathophenanthroline. No [^{14}C]ADP/ADP or [^{33}P]Pi/Pi exchange activity was detected if AtAPC1, AtAPC2 and AtAPC3 had been boiled before incorporation into liposomes or if proteoliposomes were reconstituted with sarkosyl-solubilized material from bacterial cells lacking the expression vector for the three AtAPCs or harvested immediately before induction of expression (data not shown).

The substrate specificities of AtAPC1, AtAPC2 and AtAPC3 were examined in detail by measuring the uptake of [^{14}C]ADP into proteoliposomes that had been preloaded with various potential substrates

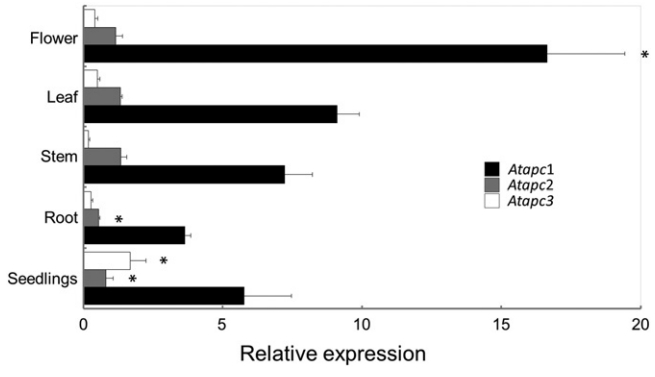

Fig. 2. Expression of *Atapc* genes in various organs. Relative expression level of *Atapc* genes in whole seedlings, root, stem, leaf and flower was analyzed by quantitative real time PCR. Relative mRNA levels of each gene were $2^{-\Delta Ct}$ calculated as described in the Materials and methods section. Black bar, *Atapc*1; gray bar, *Atapc*2; white bar, *Atapc*3. Bars represent the mean of 3 biological replicates and SEM. Asterisk indicates an organ in which the mRNA level was significantly different from that in stem by Turkey test ($p < 0.05$).

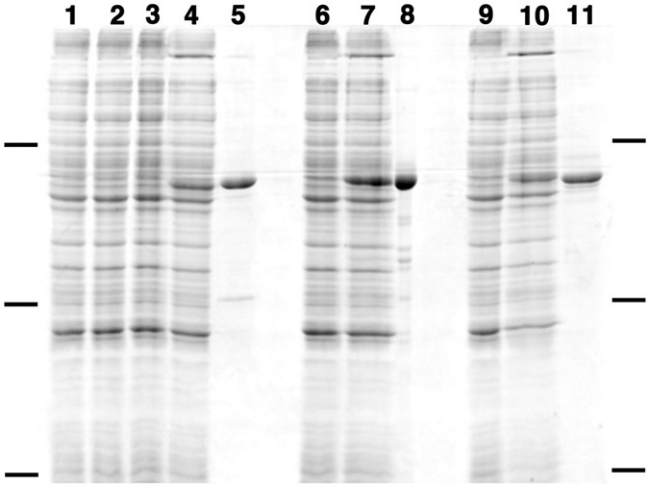

Fig. 3. Expression in *E. coli* and purification of AtAPC1, AtAPC2 and AtAPC3. Proteins were separated by SDS-PAGE and stained with Coomassie Blue. The bars flanking the gel indicate the markers (bovine serum albumin 66 kDa, carbonic anhydrase 29 kDa and cytochrome c 12 kDa). Whole *E. coli* Rosetta-gami B(DE3) cells containing the expression vector without insert (lanes 1–2), or with AtAPC1 (lanes 3–4), AtAPC2 (lanes 6–7) and AtAPC3 (lanes 9–10). Samples were taken at the time of induction (lanes 1, 3, 6 and 9) and 5 h later (lanes 2, 4, 7 and 10). Approximately 5, 6 and 4 μg of purified AtAPC1, AtAPC2 and AtAPC3, respectively, are shown in lanes 5, 8 and 11, respectively.

(Fig. 4). For all AtAPCs, the highest activities were observed in the presence of internal ADP, Pi, AMP, ATP and adenosine 5′-phosphosulfate (APS). The AtAPCs also exchanged [^{14}C]ADP with other internal substrates, although to a lesser extent: AtAPC1 with pyrophosphate,

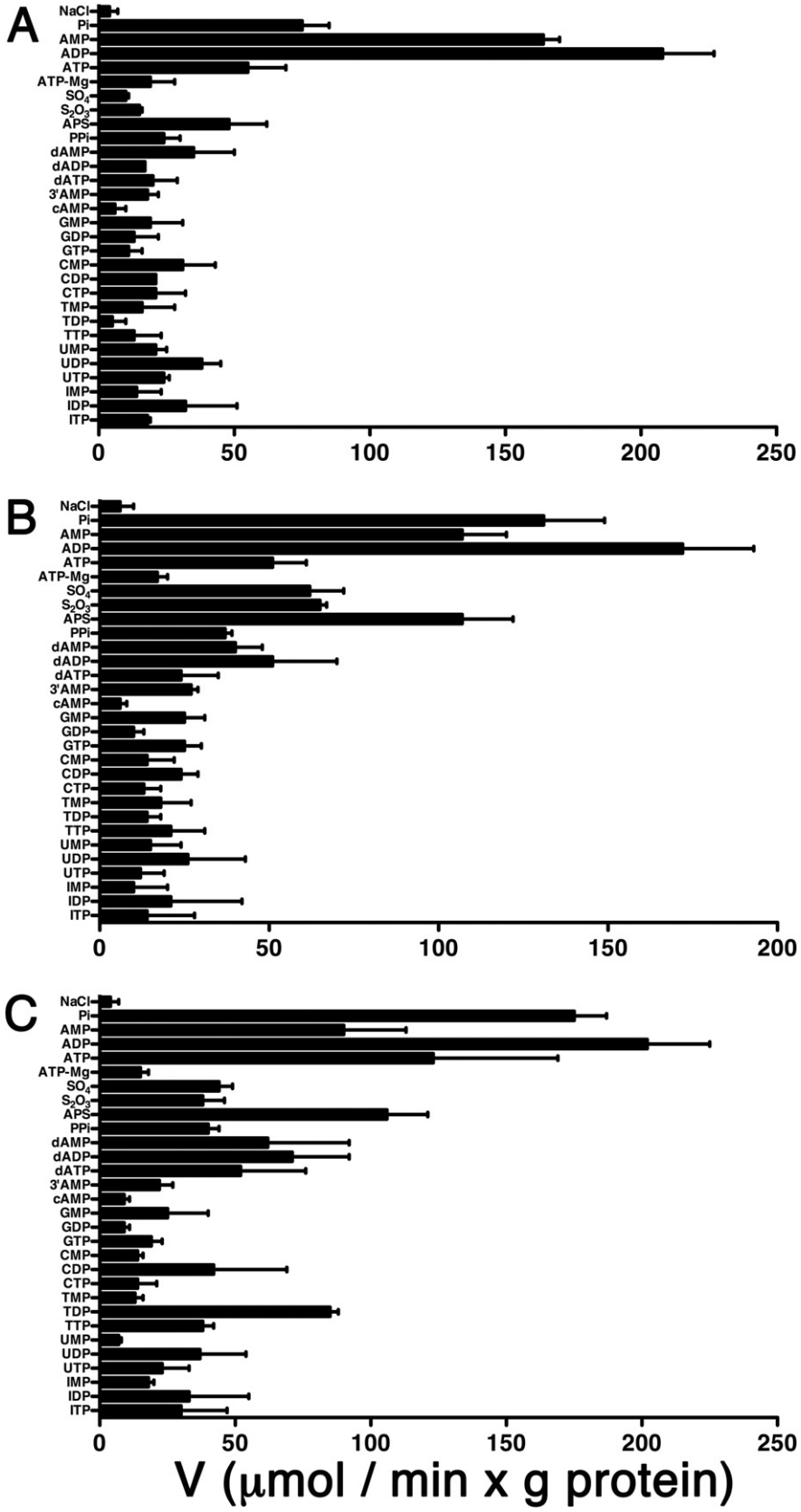

Fig. 4. Substrate specificity of AtAPC1, AtAPC2 and AtAPC3. Proteoliposomes were preloaded internally with various substrates at a concentration of 20 mM. Transport was started by the addition of 0.17 mM [^{14}C]ADP to proteoliposomes reconstituted with AtAPC1, AtAPC2 and AtAPC3, and terminated after 2 min. The transport rates of AtAPC1 (A), AtAPC2 (B) and AtAPC3 (C) are averages of at least three independent experiments in duplicate and displayed with the standard error.

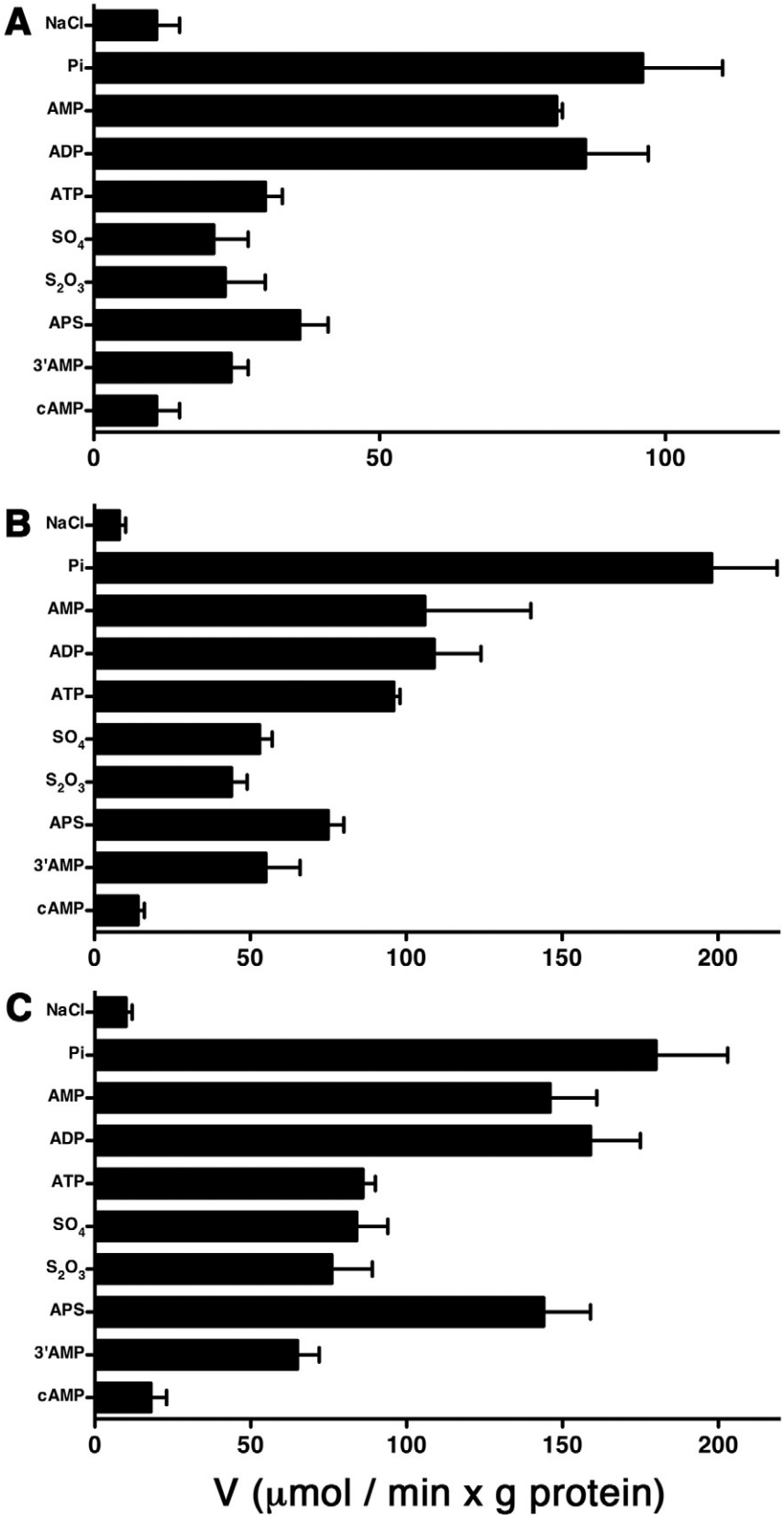

Fig. 5. Substrate specificity of AtAPC1, AtAPC2 and AtAPC3. Proteoliposomes were preloaded internally with various substrates at a concentration of 20 mM. Transport was started by the addition of 0.6 mM [^{33}P]Pi to proteoliposomes reconstituted with AtAPC1, AtAPC2 and AtAPC3, and terminated after 2 min. The transport rates of AtAPC1 (A), AtAPC2 (B) and AtAPC3 (C) are averages of at least three independent experiments in duplicate and displayed with the standard error.

dAMP, CMP, UDP, UTP and IDP (Fig. 4A); AtAPC2 with sulfate, thiosulfate, pyrophosphate, dAMP, dADP, dATP, 3′AMP, GMP, GTP, CDP, TMP, TTP, UDP and IDP (Fig. 4B); AtAPC3 with sulfate, thiosulfate, pyrophosphate, dAMP, dADP, dATP, CDP, TDP, TTP and UDP (Fig. 4C). With all three AtAPCs [^{14}C]ADP also exchanged for internal ATP–Mg at a rate significantly higher than that observed in the absence of any internal substrate (NaCl present) (Fig. 4). A very low activity was observed with most of the other G, C, T, U and I nucleotides. Furthermore, the uptake of labeled substrate was negligible with internal NaCl for all AtAPCs, with cAMP and TDP for AtAPC1, with cAMP for AtAPC2 (Fig. 4C), as well as with malate, citrate, lysine, glutamate, threonine, choline or spermine for all AtAPCs (data not shown). The substrate specificities of the AtAPCs were also examined by measuring the uptake of [^{33}P]P_i into proteoliposomes that had been preloaded with a more limited set of substrates (Fig. 5). These results basically confirm the specificity of the different AtAPCs for the substrates that were also used in the [^{14}C]ADP exchange experiments.

The [^{14}C]ADP/ADP exchange reactions catalyzed by reconstituted AtAPC1, AtAPC2 and AtAPC3 were inhibited strongly by pyridoxal-5′-phosphate, bathophenanthroline, tannic acid, $HgCl_2$, mersalyl and p-hydroxymercuribenzioate, and partially by bromcresol purple (Fig. 6). In contrast, little inhibition was observed with α-cyano-4-hydroxycinnamate and butylmalonate as well as carboxyatractyloside (strong inhibitor of the ADP/ATP carrier). N-ethylmaleimide and bongkrekic acid had little effect on AtAPC2 and AtAPC3 activity, and only partially reduced the activity of AtAPC1.

3.5. Kinetic characteristics of recombinant AtAPC proteins

In Fig. 7, A–C, the kinetics of the recombinant AtAPCs are compared for the uptake by proteoliposomes of 1 mM [^{14}C]ADP measured either as uniport (in the absence of internal ADP) or as exchange (in the presence of 20 mM ADP). The exchange reactions followed first-order kinetics, with isotopic equilibrium being approached exponentially. The rate constants and the initial rates of ADP homoexchanges deduced from the time courses [31] were 0.047, 0.047 and 0.048 min^{-1}, and 218, 206 and 261 μmol/min/g protein for AtAPC1, AtAPC2 and AtAPC3, respectively. In contrast, the uniport uptake of ADP catalyzed by the AtAPCs was very low. This mode of transport was further investigated by measuring the efflux of [^{14}C]ADP from proteoliposomes, as this provides a more sensitive assay for unidirectional transport [31]. With all three AtAPCs a low efflux of [^{14}C]ADP was observed in the absence of external substrate (Fig. 7, D–F). By contrast, addition of external P_i or ADP caused an extensive efflux of radioactively labeled ADP. These results demonstrate that AtAPC1, AtAPC2 and AtAPC3 mainly catalyze an exchange reaction of substrates.

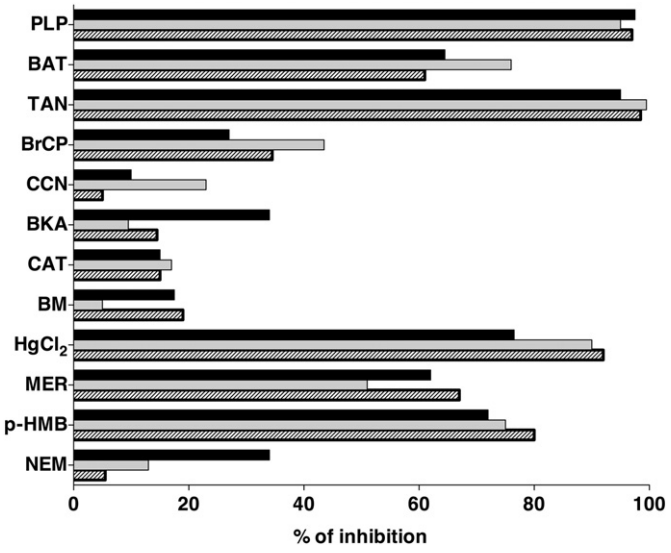

Fig. 6. Effect of inhibitors on the [^{14}C]ADP/ADP exchange by AtAPC1, AtAPC2 and AtAPC3. Proteoliposomes were preloaded internally with 20 mM ADP. Transport was initiated by adding 0.17 mM [^{14}C]ADP to proteoliposomes reconstituted with AtAPC1 (black bars), AtAPC2 (gray bars) and AtAPC3 (striped bars), and terminated after 2 min. Thiol reagents were added 2 min before the labeled substrate; the other inhibitors were added together with the labeled substrate. The final concentrations of the inhibitors were 20 mM pyridoxal 5′-phosphate (PLP), 20 mM bathophenanthroline (BAT), 0.2% tannic acid (TAN), 0.3 mM bromcresol purple (BrCP), 1 mM α-cyano-4-hydroxycinnamate (CCN), 10 μM bongkrekic acid (BKA), 10 μM carboxyatractyloside (CAT), 2 mM butylmalonate (BM), 0.2 mM mercury chloride ($HgCl_2$), 0.1 mM mersalyl (MER), 0.1 mM p-hydroxymercuribenzoate (p-HMB), and 1 mM N-ethylmaleimide (NEM). The extent of inhibition in percent was calculated from the average of at least three independent experiments.

The kinetic constants of AtAPC1, AtAPC2 and AtAPC3 were determined from the initial transport rate of homo-exchanges at various external labeled substrate concentrations in the presence of a constant saturating internal substrate concentration of 20 mM (Table 1). The half-saturation constants (K_m) of all three recombinant proteins for adenine nucleotides were between 0.08 and 0.32 mM, values that were lower than the K_m for P_i, which ranged between 0.60 and 0.74 mM. Furthermore, the K_m values for AMP were slightly higher than those for ADP and ATP for all three AtAPCs. The maximal activities (V_{max}) of AtAPCs for adenine nucleotides and P_i varied between 300 and 410 μmol/min/g with the exception of the V_{max} of AtAPC1 for P_i and ATP, and that of AtAPC2 for AMP and ATP, which were lower.

3.6. Influence of Ca^{2+} on the activity of AtAPCs

Binding of radioactive Ca^{2+} to AtAPC1, AtAPC2 and AtAPC3 has already been demonstrated [23]. Here the effect of Ca^{2+} and of the divalent ion chelators EGTA and EDTA in de-ionized ultrapure water on the transport rates of AtAPC1, AtAPC2 and AtAPC3 was investigated (Fig. 8, A–C). The activities of AtAPCs were slightly increased by the addition of $CaCl_2$ and diminished by the addition of EGTA and EDTA. In the presence of 0.5 mM EDTA and 1 mM $CaCl_2$, the activity was re-established. These results indicate that the low concentration of Ca^{2+} present in the reconstitution mixture (probably derived from egg yolk phospholipids and small contaminants in the buffers and salts) is sufficient for significant transport activity and that the addition of Ca^{2+} chelators reduces the concentration of free Ca^{2+} causing inhibition of transport, which can be restored by the presence of additional Ca^{2+}.

The Ca^{2+}-dependence of the transport activities of AtAPC1, AtAPC2 and AtAPC3 was further investigated by measuring the transport rates as a function of the free Ca^{2+} concentration (Fig. 8, D–F). All three AtAPCs were highly Ca^{2+}-sensitive with a half-maximal activation of about 0.2, 0.2 and 0.8 μM for AtAPC1, AtAPC2 and AtAPC3, respectively.

4. Discussion

Considering their C-terminal domains, the percentage of identical amino acids between the AtAPCs and the human APCs (46–48%) or the *S. cerevisiae* APC Sal1p (21–24%) does not allow one to make reliable assumptions on the substrate specificity or the transport modes of the Arabidopsis proteins. In fact, i) the basic amino acid identity existing between the different members of the mitochondrial carrier family in plants and humans is rather high (about 12%) and ii) even clear isoforms of MCs such as the human ornithine carriers 1 and 2 sharing 87% identical amino acid, display substantial differences in the substrate specificity and kinetic parameters [25,46]. Furthermore, until now the identification of the AtAPCs as ATP–Mg/Pi carriers relies only on their ability to partly complement the growth defect of *S. cerevisiae* cells lacking Sal1p [23], whose biochemical characterization is limited to the demonstration that this protein is able to transport ATP and ADP [47]. For these reasons we decided to thoroughly analyze the biochemical properties of the three Arabidopsis recombinant AtAPCs upon expression in *E. coli*, purification and reconstitution into liposomes.

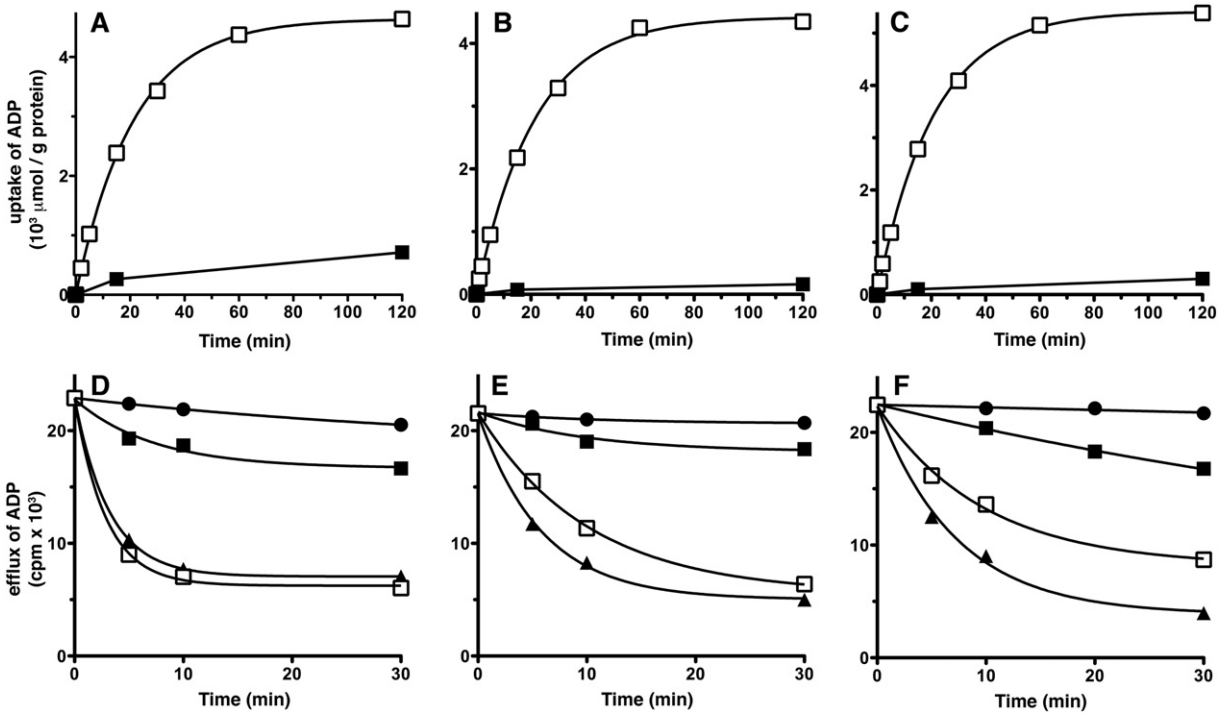

Fig. 7. Kinetics of exchange reactions catalyzed by AtAPC1, AtAPC2 and AtAPC3. Proteoliposomes were reconstituted with AtAPC1 (A and D), AtAPC2 (B and E) and AtAPC3 (C and F). A–C, 1 mM [^{14}C]ADP was added to proteoliposomes containing 20 mM ADP (unfilled squares) or 20 mM NaCl (filled squares). D–F, proteoliposomes with 5 mM ADP internally were loaded with [^{14}C]ADP by carrier-mediated exchange equilibrium. After removal of the external substrate by Sephadex G-75, the efflux of [^{14}C]ADP was started by addition of 5 mM ADP (triangles), 5 mM Pi (unfilled squares), 5 mM NaCl (filled squares) or 5 mM ADP, 20 mM pyridoxal 5′-phosphate and 20 mM bathophenanthroline (filled circles). Similar results were obtained in at least three independent experiments.

The three AtAPCs all transport P_i, AMP, ADP, ATP and APS, and, to a lesser extent, deoxy-adenine nucleotides and other nucleotides, but none of the many other compounds that have been tested (Figs. 4 and 5). However, there are some differences in the transport properties of the AtAPCs. For example, at variance with AtAPC1, AtAPC2 and AtAPC3 also transport sulfate and thiosulfate, and catalyze a higher transport exchange rate of Pi/ADP and APS/ADP (Figs. 4 and 5). The V_{max} values of AtAPC1 for Pi/Pi exchange are lower than those of AtAPC2 and AtAPC3, whereas the V_{max} values of AtAPC3 for ATP/ATP exchange are higher than those of AtAPC1 and AtAPC2. Furthermore, the K_m values of AtAPC1 for ATP are higher than those of AtAPC2 and AtAPC3. In addition, *N*-ethylmaleimide and bongkrekic acid are more effective inhibitors of AtAPC1 than of AtAPC2 and AtAPC3, whereas α-cyano-4-hydroxycinnamate is more effective on AtAPC2 than on AtAPC1 and AtAPC3. The greater inhibition of AtAPC1 by *N*-ethylmaleimide might be explained by the presence of a specific cysteine (C356) in AtAPC1 (Supplementary Fig. S1), a residue which is not present in the other AtAPCs. In contrast, the reason(s) why bongkrekic acid and α-cyano-4-hydroxycinnamate exhibit a higher inhibitory potency on AtAPC1 and AtAPC2, respectively, are currently unclear.

Table 1
Kinetic constants of recombinant AtAPC1, AtAPC2 and AtAPC3. The values were calculated from initial rates of homo-exchange under variation of the external substrate concentration. The exchange was started by the addition of appropriate concentrations of labeled substrate to proteoliposomes preloaded internally with the same substrate at 20 mM. The reaction time was 2 min for AtAPC1, AtAPC2 and AtAPC3.

Carrier and substrate	K_m (mM)	V_{max} (µmol/min × g protein)
AtAPC1		
Pi	0.70 ± 0.03	100 ± 30
AMP	0.32 ± 0.08	320 ± 10
ADP	0.18 ± 0.01	380 ± 40
ATP	0.19 ± 0.01	54 ± 16
AtAPC2		
Pi	0.74 ± 0.18	380 ± 120
AMP	0.25 ± 0.01	150 ± 50
ADP	0.16 ± 0.02	350 ± 130
ATP	0.08 ± 0.03	54 ± 20
AtAPC3		
Pi	0.60 ± 0.10	330 ± 60
AMP	0.25 ± 0.03	300 ± 80
ADP	0.17 ± 0.02	410 ± 70
ATP	0.14 ± 0.03	330 ± 120

The substrate specificity of AtAPCs is different from that of any other mitochondrial carrier subfamilies [10,11]. It also differs from the recently characterized MC YPR011cp from *S. cerevisiae* which shares 29–35% identical residues with the C-terminal domains of the AtAPCs and transports APS, sulfate and phosphate but not ATP or ADP [48]. The transport of APS is intriguing given that it is a key intermediate of the sulfur assimilation pathway, which leads to the biosynthesis of cysteine, methionine and glutathione [49]. In plants APS is synthesized in the cytosol and in plastids, but not in mitochondria, whereas the enzymes necessary for converting APS to cysteine exist in the cytosol, plastids and mitochondria [50]. Therefore, APS imported into mitochondria by the AtAPCs may be used for mitochondrial cysteine biosynthesis, and therefore its requirement in the mitochondrial matrix could well increase as a means by which to enhance the synthesis of glutathione under conditions of stress [49].

The substrate specificities and transport properties of AtAPCs described in the present work resemble those of the only other well-characterized members of the APC-subfamily of mitochondrial carriers, i.e. the human APCs [19], with the following major differences: i) AtAPCs display a small but reproducible uniport, i.e. a substrate efflux from loaded proteoliposomes in the absence of externally-added substrate (Fig. 7), unlike the human APCs, ii) the affinities of AtAPCs for P_i, AMP, ADP and ATP as evaluated from the K_m values are all higher than those of the human APCs, iii) AtAPCs transport ATP–Mg at a rate lower than ATP (Fig. 4), iv) pyridoxal 5′-phosphate inhibits all AtAPCs

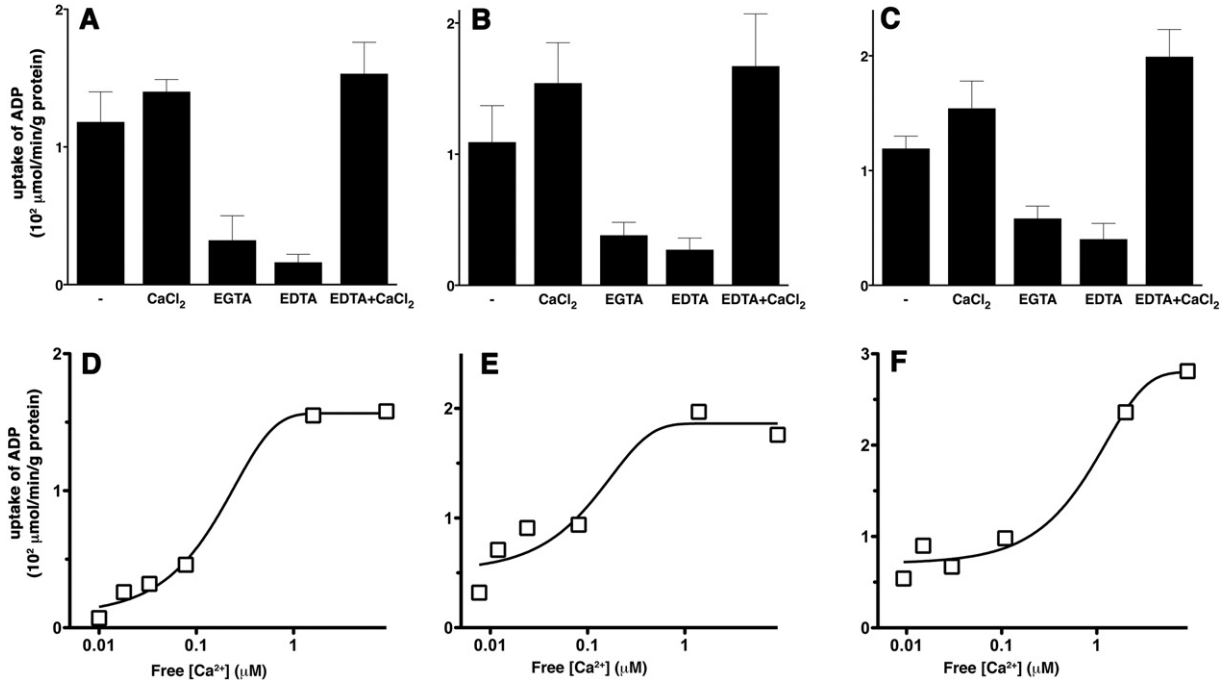

Fig. 8. Effect of Ca^{2+} on the transport activities of AtAPC1, AtAPC2 and AtAPC3. Proteoliposomes were reconstituted with AtAPC1 (A and D), AtAPC2 (B and E) and AtAPC3 (C and F). A–C, the [^{14}C]ADP/ADP transport rates were measured in de-ionized ultrapure water without additions (−) or with addition of 1 mM $CaCl_2$, 0.5 mM EGTA, 0.5 mM EDTA or both 0.5 mM EDTA and 1 mM $CaCl_2$. The average transport rates were calculated from the average of at least three independent experiments and displayed with the standard error. D–F, dependence of AtAPCs activities on the free Ca^{2+} concentration. The [^{14}C]ADP/ADP transport rates were measured in de-ionized ultrapure water in the presence of 0.5 mM EDTA and various concentrations of Ca^{2+}. Similar results were obtained in at least three independent experiments.

and only APC2 in humans, whereas bromcresol purple inhibits poorly the AtAPCs and strongly the human APCs, and v) the ability of the human APCs to transport APS, sulfate and thiosulfate has not yet been ascertained.

The transport activity of AtAPC1, AtAPC2 and AtAPC3 has been demonstrated to be Ca^{2+}-dependent (Fig. 8). It is probably the first time that the Ca^{2+}-dependence of APC transport activity is demonstrated in a reconstituted in vitro system with purified proteins. The presence of the EF hand Ca^{2+}-binding motifs in the N-terminal domains of the three AtAPCs suggests that the transport activity of these carriers is regulated by the interaction between Ca^{2+} and their N-terminal domain. The relationship between the free Ca^{2+} concentration and the transport activity observed here (Fig. 8) could be explained either by the presence, under our experimental conditions, of EDTA and consequent depletion of added Ca^{2+} at lower concentrations or by a cooperative effect of Ca^{2+} binding to the four different binding sites in the N-terminal domain of the APCs in a similar way to what has been suggested for other multiple EF hand domains [51]. The half-maximal activation of the AtAPCs' transport rate by free Ca^{2+} ranges from 0.2 and 0.8 µM, a value which is lower than that (about 3–15 µM) determined in experiments with mitochondria from different sources [18,47,52–54]. The amount of free Ca^{2+} required to activate AtAPCs is also lower than that reported to induce conformational changes in the N-terminal domain of the human APC1 in vitro [24]. The higher sensitivity of AtAPCs to Ca^{2+} than that of their homologues from animals and yeast might be explained by the fact that plant cells have a lower concentration of Ca^{2+} in the cytoplasm (about 0.1 µM) [55].

The results from qRT-PCR and promoter-GUS analyses indicate that AtAPC1 is the dominant APC isoform in *A. thaliana*. This observation is consistent with the publicly available data in eFP browser [56]. Although very little GUS activity was detected from *Atapc2* and *Atapc3* promoters most likely due to low expression levels of these genes, at least *Atapc1* and *Atapc2* should be specifically expressed in vascular tissues in aerial part. Furthermore, the expression levels of AtAPC1 and AtAPC3 have been shown to fluctuate in conditions of stress due to pathogen infection and upon mitochondrial dysfunction as well as being highly responsive on cold and dehydration-related stresses [57–59]. Thus, the AtAPCs are regulated at transcriptional level by being expressed constitutively and upon induction, as well as directly by their sensitivity to Ca^{2+}, which in turn is controlled by biotic and abiotic signals. Ca^{2+} signaling in plants is thought to play a role in response to different stimuli like drought, salt or osmotic stresses, temperature, light, plant hormones and pathogens [60]. The second messenger Ca^{2+} has many targets in plants because the genome of *A. thaliana* encodes at least 250 EF-hand proteins compared with 132 in *Drosophila melanogaster* and 83 in humans [61]. Indeed the association of Ca^{2+} is not without precedence in plant mitochondrial energy metabolism since some of the NADH dehydrogenases important in alternative pathways of plant respiration, which are envoked under conditions of stress [62], are also Ca^{2+}-dependent.

Given the tissue distribution and the regulation of AtAPCs' expression, the presence of Ca^{2+} sensors in the AtAPCs and their ability to exchange adenine nucleotides for P_i (or, in the case of AtAPC2 and AtAPC3, sulfate), the main physiological role of AtAPCs is probably to modulate the adenine nucleotide concentration in the mitochondria. In mammalian systems, the APC isoforms have been associated with cell-type- or physiological-condition-specific functions by regulating metabolic pathways that have adenine nucleotide-dependent enzymes compartmentalized in the mitochondrial matrix, including oxidative phosphorylation, gluconeogenesis and urea biosynthesis [18,19,53,54,63]. While several metabolic pathways differ between animals and plants, for example the early steps of plant gluconeogenesis are not dependent on ATP [64], it is likely that citrulline biosynthesis, action of the ADP/ATP carrier and F_0F_1 ATPase as well as mitochondrial DNA replication, transcription and protein synthesis and the import of nuclear encoded proteins, are all regulated in plants by these transporters. In particular, the role of AtAPCs is likely to be highly important in conditions under which the mitochondrial adenine nucleotide pool is adaptively and specifically varied with respect to the whole cell adenine nucleotide content such as has been documented for the light–dark

transition in wheat [65]. As has been described in mammals [18,19], net import of adenine nucleotides into the mitochondria is likely prominent in tissues wherein expression of the APCs is considerably elevated. Looking into their expression at an organ by organ basis reveals that AtAPC1 and AtAPC3 are highly expressed in tissues such as embryos and pollen which are characterized to have high energetic requirements to sustain elevated rates of biosynthesis and growth [66,67], with pollen growth additionally being highly dependent on the second messenger Ca^{2+} [68]. Shoots and roots also displayed relatively high values of AtAPCs as would perhaps be anticipated given the need for ATP in early seedling development and to sustain root growth energetically [69,70]. AtAPC2 is more or less constitutively expressed, suggesting that some residual activity of AtAPCs is required for normal cellular operation. The conditionally expressed AtAPCs also appear to be highly important under conditions of stress particularly cold stress but also under conditions which lead to dehydration. Given that all conditions have been characterized to involve metabolic reprogramming resulting in the accumulation of compatible solutes [71], it is tempting to speculate that AtAPC3 is involved in mediating the influx of adenine nucleotides to support the high rates of mitochondrially-related osmoprotectant synthesis.

In summary, we demonstrated here that the three Arabidopsis mitochondrial AtAPCs are capable of transporting phosphate, AMP, ADP, ATP, adenosine 5′-phosphosulfate and, to a lesser extent, other nucleotides and that AtAPC2 and AtAPC3 also have the ability to transport sulfate and thiosulfate. As the mitochondria additionally possess specific transporters for phosphate and sulfate it is conceivable that their transport also takes part in the net influx of adenine nucleotides under conditions where the concentrations of these nucleotides limit mitochondrial biosynthesis. The data presented here also reveal that the mitochondrial AtAPCS are regulated at the transcriptional level and by Ca^{2+}, and indicate an important role for these transporters under cold stress and other conditions which result in dehydration as well as in fast growing tissues such as pollen tubes and root tips. Future experiments relying on reverse genetics will be required to pinpoint the exact in vivo roles of each of the mitochondrial AtAPCs.

Transparency document

The Transparency document associated with this article can be found, in the online version.

Acknowledgments

This work was supported by grants from the Ministero dell'Università e della Ricerca (MIUR), the Center of Excellence on Comparative Genomics, Apulia Region, and the Italian Human ProteomeNet no. RBRN07BMCT_009 (MIUR) as well as from the Max-Planck-Gesellschaft.

Appendix A. Supplementary data

Supplementary data to this article can be found online at http://dx.doi.org/10.1016/j.bbabio.2015.06.015.

References

[1] F. Palmieri, The mitochondrial transporter family SLC25: identification, properties and physiopathology, Mol. Asp. Med. 34 (2013) 465–484.
[2] F. Palmieri, Mitochondrial transporters of the SLC25 family and associated diseases: a review, J. Inherit. Metab. Dis. 37 (2014) 565–575.
[3] A. Vozza, G. Parisi, F. De Leonardis, F.M. Lasorsa, A. Castegna, D. Amorese, et al., UCP2 transports C4 metabolites out of mitochondria, regulating glucose and glutamine oxidation, Proc. Natl. Acad. Sci. U. S. A. 111 (2014) 960–965.
[4] V. Porcelli, G. Fiermonte, A. Longo, F. Palmieri, The human gene SLC25A29, of solute carrier family 25, encodes a mitochondrial transporter of basic amino acids, J. Biol. Chem. 289 (2014) 13374–13384.
[5] M. Saraste, J.E. Walker, Internal sequence repeats and the path of polypeptide in mitochondrial ADP/ATP translocase, FEBS Lett. 144 (1982) 250–254.
[6] F. Palmieri, Mitochondrial carrier proteins, FEBS Lett. 346 (1994) 48–54.
[7] E. Pebay-Peyroula, C. Dahout-Gonzalez, R. Kahn, V. Trézéguet, G.J.-M. Lauquin, G. Brandolin, Structure of mitochondrial ADP/ATP carrier in complex with carboxyatractyloside, Nature 426 (2003) 39–44.
[8] J.J. Ruprecht, A.M. Hellawell, M. Harding, P.G. Crichton, A.J. McCoy, E.R.S. Kunji, Structures of yeast mitochondrial ADP/ATP carriers support a domain-based alternating-access transport mechanism, Proc. Natl. Acad. Sci. U. S. A. 111 (2014) E426–E434.
[9] F. Palmieri, C.L. Pierri, Structure and function of mitochondrial carriers — role of the transmembrane helix P and G residues in the gating and transport mechanism, FEBS Lett. 584 (2010) 1931–1939.
[10] F. Palmieri, C.L. Pierri, Mitochondrial metabolite transport, Essays Biochem. 47 (2010) 37–52.
[11] F. Palmieri, C.L. Pierri, A. De Grassi, A. Nunes-Nesi, A.R. Fernie, Evolution, structure and function of mitochondrial carriers: a review with new insights, Plant J. 66 (2011) 161–181.
[12] M. Klingenberg, The ADP and ATP transport in mitochondria and its carrier, Biochim. Biophys. Acta 1778 (2008) 1978–2021.
[13] I. Haferkamp, J.H.P. Hackstein, F.G.J. Voncken, G. Schmit, J. Tjaden, Functional integration of mitochondrial and hydrogenosomal ADP/ATP carriers in the *Escherichia coli* membrane reveals different biochemical characteristics for plants, mammals and anaerobic chytrids, Eur. J. Biochem. 269 (2002) 3172–3181.
[14] A.H. Millar, J.L. Heazlewood, Genomic and proteomic analysis of mitochondrial carrier proteins in Arabidopsis, Plant Physiol. 131 (2003) 443–453.
[15] V. Dolce, V. Iacobazzi, F. Palmieri, J.E. Walker, The sequences of human and bovine genes of the phosphate carrier from mitochondria contain evidence of alternatively spliced forms, J. Biol. Chem. 269 (1994) 10451–10460.
[16] G. Fiermonte, V. Dolce, F. Palmieri, Expression in Escherichia coli, functional characterization, and tissue distribution of isoforms A and B of the phosphate carrier from bovine mitochondria, J. Biol. Chem. 273 (1998) 22782–22787.
[17] L. Palmieri, A. Santoro, F. Carrari, E. Blanco, A. Nunes-Nesi, R. Arrigoni, et al., Identification and characterization of ADNT1, a novel mitochondrial adenine nucleotide transporter from Arabidopsis, Plant Physiol. 148 (2008) 1797–1808.
[18] J.R. Aprille, Mechanism and regulation of the mitochondrial ATP–Mg/P(i) carrier, J. Bioenerg. Biomembr. 25 (1993) 473–481.
[19] G. Fiermonte, F. De Leonardis, S. Todisco, L. Palmieri, F.M. Lasorsa, F. Palmieri, Identification of the mitochondrial ATP–Mg/Pi transporter. Bacterial expression, reconstitution, functional characterization, and tissue distribution, J. Biol. Chem. 279 (2004) 30722–30730.
[20] L. Palmieri, B. Pardo, F.M. Lasorsa, A. del Arco, K. Kobayashi, M. Iijima, et al., Citrin and aralar1 are Ca(2+)-stimulated aspartate/glutamate transporters in mitochondria, EMBO J. 20 (2001) 5060–5069.
[21] F.M. Lasorsa, P. Pinton, L. Palmieri, G. Fiermonte, R. Rizzuto, F. Palmieri, Recombinant expression of the Ca(2+)-sensitive aspartate/glutamate carrier increases mitochondrial ATP production in agonist-stimulated Chinese hamster ovary cells, J. Biol. Chem. 278 (2003) 38686–38692.
[22] J. Traba, J. Satrústegui, A. del Arco, Characterization of SCaMC-3-like/slc25a41, a novel calcium-independent mitochondrial ATP–Mg/Pi carrier, Biochem. J. 418 (2009) 125–133.
[23] S. Stael, A.G. Rocha, A.J. Robinson, P. Kmiecik, U.C. Vothknecht, M. Teige, Arabidopsis calcium-binding mitochondrial carrier proteins as potential facilitators of mitochondrial ATP-import and plastid SAM-import, FEBS Lett. 585 (2011) 3935–3940.
[24] Q. Yang, S. Brüschweiler, J.J. Chou, A self-sequestered calmodulin-like Ca(2+) sensor of mitochondrial SCaMC carrier and its implication to Ca(2+)-dependent ATP–Mg/Pi transport, Structure 22 (2014) 209–217.
[25] M. Monné, D.V. Miniero, L. Daddabbo, A.J. Robinson, E.R. Kunji, F. Palmieri, Substrate specificity of the two mitochondrial ornithine carriers can be swapped by single mutation in substrate binding site, J. Biol. Chem. 287 (2012) 7925–7934.
[26] T. Murashige, F. Skoog, A revised medium for rapid growth and bioassays with tobacco tissue cultures, Physiol. Plant. 15 (1962) 735–743.
[27] S.J. Clough, A.F. Bent, Floral dip: a simplified method for *Agrobacterium*-mediated transformation of *Arabidopsis thaliana*, Plant J. 16 (1998) 735–743.
[28] T. Czechowski, M. Stitt, T. Altmann, M.K. Udvardi, W.-R. Scheible, Genome-wide identification and testing of superior reference genes for transcript normalization in Arabidopsis, Plant Physiol. 139 (2005) 5–17.
[29] C.M. Marobbio, G. Agrimi, F.M. Lasorsa, F. Palmieri, Identification and functional reconstitution of yeast mitochondrial carrier for S-adenosylmethionine, EMBO J. 22 (2003) 5975–5982.
[30] G. Agrimi, A. Russo, P. Scarcia, F. Palmieri, The human gene SLC25A17 encodes a peroxisomal transporter of coenzyme A, FAD and NAD+, Biochem. J. 443 (2012) 241–247.
[31] F. Palmieri, C. Indiveri, F. Bisaccia, V. Iacobazzi, Mitochondrial metabolite carrier proteins: purification, reconstitution, and transport studies, Methods Enzymol. 260 (1995) 349–369.
[32] M.E. Hoyos, L. Palmieri, T. Wertin, R. Arrigoni, J.C. Polacco, F. Palmieri, Identification of a mitochondrial transporter for basic amino acids in *Arabidopsis thaliana* by functional reconstitution into liposomes and complementation in yeast, Plant J. 33 (2003) 1027–1035.
[33] L. Palmieri, R. Arrigoni, E. Blanco, F. Carrari, M.I. Zanor, C. Studart-Guimaraes, et al., Molecular identification of an Arabidopsis S-adenosylmethionine transporter. Analysis of organ distribution, bacterial expression, reconstitution into liposomes, and functional characterization, Plant Physiol. 142 (2006) 855–865.
[34] L. Palmieri, N. Picault, R. Arrigoni, E. Besin, F. Palmieri, M. Hodges, Molecular identification of three *Arabidopsis thaliana* mitochondrial dicarboxylate carrier isoforms: organ distribution, bacterial expression, reconstitution into liposomes and functional characterization, Biochem. J. 410 (2008) 621–629.

[35] G. Fiermonte, V. Dolce, L. Palmieri, M. Ventura, M.J. Runswick, F. Palmieri, et al., Identification of the human mitochondrial oxodicarboxylate carrier. Bacterial expression, reconstitution, functional characterization, tissue distribution, and chromosomal location, J. Biol. Chem. 276 (2001) 8225–8230.
[36] L. Palmieri, F.M. Lasorsa, V. Iacobazzi, M.J. Runswick, F. Palmieri, J.E. Walker, Identification of the mitochondrial carnitine carrier in *Saccharomyces cerevisiae*, FEBS Lett. 462 (1999) 472–476.
[37] S. Floyd, C. Favre, F.M. Lasorsa, M. Leahy, G. Trigiante, P. Stroebel, A. Marx, G. Loughran, K. O'Callaghan, C.M. Marobbio, D.J. Slotboom, E.R. Kunji, F. Palmieri, R. O'Connor, The insulin-like growth factor-I-mTOR signaling pathway induces the mitochondrial pyrimidine nucleotide carrier to promote cell growth, Mol. Biol. Cell 18 (2007) (3545-3455).
[38] G. Fiermonte, E. Paradies, S. Todisco, C.M.T. Marobbio, F. Palmieri, A novel member of solute carrier family 25 (SLC25A42) is a transporter of coenzyme A and adenosine 3′,5′-diphosphate in human mitochondria, J. Biol. Chem. 284 (2009) 18152–18159.
[39] A. Castegna, P. Scarcia, G. Agrimi, L. Palmieri, H. Rottensteiner, I. Spera, et al., Identification and functional characterization of a novel mitochondrial carrier for citrate and oxoglutarate in *S. cerevisiae*, J. Biol. Chem. 285 (2010) 17359–17370.
[40] F. Palmieri, B. Rieder, A. Ventrella, E. Blanco, P.T. Do, A. Nunes-Nesi, et al., Molecular identification and functional characterization of *Arabidopsis thaliana* mitochondrial and chloroplastic NAD+ carrier proteins, J. Biol. Chem. 284 (2009) 31249–31259.
[41] C.M.T. Marobbio, M.A. Di Noia, F. Palmieri, Identification of a mitochondrial transporter for pyrimidine nucleotides in *Saccharomyces cerevisiae*: bacterial expression, reconstitution and functional characterization, Biochem. J. 393 (2006) 441–446.
[42] C. Indiveri, V. Iacobazzi, N. Giangregorio, F. Palmieri, Bacterial overexpression, purification, and reconstitution of the carnitine/acylcarnitine carrier from rat liver mitochondria, Biochem. Biophys. Res. Commun. 249 (1998) 589–594.
[43] L. Capobianco, F. Bisaccia, M. Mazzeo, F. Palmieri, The mitochondrial oxoglutarate carrier: sulfhydryl reagents bind to cysteine-184, and this interaction is enhanced by substrate binding, Biochemistry 35 (1996) 8974–8980.
[44] K. Toufighi, S.M. Brady, R. Austin, E. Ly, N.J. Provart, The botany array resource: e-Northerns, expression angling, and promoter analyses, Plant J. 43 (2005) 153–163.
[45] T. Obayashi, S. Hayashi, M. Saeki, H. Ohta, K. Kinoshita, ATTED-II provides coexpressed gene networks for Arabidopsis, Nucleic Acids Res. 37 (2009) D987–D991.
[46] G. Fiermonte, V. Dolce, L. David, F.M. Santorelli, C. Dionisi-Vici, F. Palmieri, J.E. Walker, The mitochondrial ornithine transporter. Bacterial expression, reconstitution, functional characterization, and tissue distribution of two human isoforms, J. Biol. Chem. 278 (2003) 32778–32783.
[47] J. Traba, E.M. Froschauer, G. Wiesenberger, J. Satrústegui, A. Del Arco, Yeast mitochondria import ATP through the calcium-dependent ATP–Mg/Pi carrier Sal1p, and are ATP consumers during aerobic growth in glucose, Mol. Microbiol. 69 (2008) 570–585.
[48] S. Todisco, M.A. Di Noia, A. Castegna, F.M. Lasorsa, E. Paradies, F. Palmieri, The *Saccharomyces cerevisiae* gene YPR011c encodes a mitochondrial transporter of adenosine 5′-phosphosulfate and 3′-phospho adenosine 5′-phosphosulfate, Biochim. Biophys. Acta 1837 (2014) 326–334.
[49] S. Kopriva, S.G. Mugford, P. Baraniecka, B.R. Lee, C.A. Matthewman, A. Koprivova, Control of sulfur partitioning between primary and secondary metabolism in Arabidopsis, Front. Plant Sci. 19 (2012) 163.
[50] J.E. Lunn, M. Droux, J. Martin, R. Douce, Localization of ATP sulfurylase and O-acetylserine(thiol)lyase in spinach leaves, Plant Physiol. 94 (1990) 1345–1352.
[51] J.L. Gifford, M.P. Walsh, H.J. Vogel, Structures and metal-ion-binding properties of the Ca2+-binding helix–loop–helix EF-hand motifs, Biochem. J. 405 (2007) 199–221.
[52] M.T. Nosek, D.T. Dransfield, J.R. Aprille, Calcium stimulates ATP–Mg/Pi carrier activity in rat liver mitochondria, J. Biol. Chem. 265 (1990) 8444–8450.
[53] J. Traba, A. Del Arco, M.R. Duchen, G. Szabadkai, J. Satrústegui, SCaMC-1 promotes cancer cell survival by desensitizing mitochondrial permeability transition via ATP/ADP-mediated matrix Ca(2+) buffering, Cell Death Differ. 19 (2012) 650–660.
[54] I. Amigo, J. Traba, M.M. González-Barroso, C.B. Rueda, M. Fernández, E. Rial, A. Sánchez, J. Satrústegui, A. Del Arco, Glucagon regulation of oxidative phosphorylation requires an increase in matrix adenine nucleotide content through Ca2+ activation of the mitochondrial ATP–Mg/Pi carrier SCaMC-3, J. Biol. Chem. 288 (2013) 7791–7802.
[55] S. Stael, B. Wurzinger, A. Mair, N. Mehlmer, U.C. Vothknecht, M. Teige, Plant organellar calcium signalling: an emerging field, J. Exp. Bot. 63 (2012) 1525–1542.
[56] D. Winter, B. Vinegar, H. Nahal, R. Ammar, G.V. Wilson, N.J. Provart, An "Electronic Fluorescent Pictograph" browser for exploring and analyzing large-scale biological data sets, PLoS One 2 (2007) (e718).
[57] H.-G. Kang, C.-S. Oh, M. Sato, F. Katagiri, J. Glazebrook, H. Takahashi, et al., Endosome-associated CRT1 functions early in resistance gene-mediated defense signaling in Arabidopsis and tobacco, Plant Cell 22 (2010) 918–936.
[58] X. Wang, J.N. Culver, DNA binding specificity of ATAF2, a NAC domain transcription factor targeted for degradation by tobacco mosaic virus, BMC Plant Biol. 12 (2012) 157.
[59] A.L. Umbach, J. Zarkovic, J. Yu, M.E. Ruckle, L. McIntosh, J.J. Hock, et al., Comparison of intact *Arabidopsis thaliana* leaf transcript profiles during treatment with inhibitors of mitochondrial electron transport and TCA cycle, PLoS One 7 (2012) (e44339).
[60] O. Batistič, J. Kudla, Analysis of calcium signaling pathways in plants, Biochim. Biophys. Acta 1820 (2012) 1283–1293.
[61] I.S. Day, V.S. Reddy, G. Shad Ali, A.S.N. Reddy, Analysis of EF-hand-containing proteins in Arabidopsis, Genome Biol. 3 (2002) (RESEARCH0056).
[62] D.A. Geisler, C. Broselid, L. Hederstedt, A.G. Rasmusson, Ca2+-binding and Ca2+ independent respiratory NADH and NADPH dehydrogenases of *Arabidopsis thaliana*, J. Biol. Chem. 282 (2007) 28455–28464.
[63] R.P. Anunciado-Koza, J. Zhang, J. Ukropec, S. Bajpeyi, R.A. Koza, R.C. Rogers, W.T. Cefalu, R.L. Mynatt, L.P. Kozak, Inactivation of the mitochondrial carrier SLC25A25 (ATP–Mg^{2+}/Pi transporter) reduces physical endurance and metabolic efficiency in mice, J. Biol. Chem. 286 (2011) 11659–11671.
[64] P. Eastmond, H. Astley, K. Parsley, S. Aubry, B. Williams, C. Craddock, A. Nunes-Nesi, A.R. Fernie, J.M. Hibberd, Arabidopsis uses two gluconeogenic gateways for organic acids to fuel seedling establishment, Nat. Commun. (2014)http://dx.doi.org/10.1038/ncomms7659 (in press).
[65] M. Stitt, R. Lilley, H.W. Heldt, Adenine nucleotide levels in the cytosol, chloroplasts and mitochondria of wheat leaf protoplasts, Plant Physiol. 70 (1982) 971–977.
[66] G. Obermeyer, L. Fragner, V. Lang, W. Weckwerth, Dynamic adaptation of metabolic pathways during germination and growth of lily pollen tubes after inhibition of the electron transport chain, Plant Physiol. 162 (2013) 1822–1833.
[67] K. Weigelt, H. Küster, R. Radchuk, M. Müller, H. Weichert, A. Fait, A.R. Fernie, I. Saalbach, H. Weber, Increasing amino acid supply in pea embryos reveals specific interactions of N and C metabolism, and highlight the importance of mitochondrial metabolism, Plant J. 55 (2008) 909–926.
[68] L. Steinhorst, J. Kulda, Calcium — a central regulator of pollen germination and tube growth, Biochim. Biophys. Acta, Mol. Cell Res. 1833 (2013) 1573–1581.
[69] N. Linka, F.L. Theodoulou, R. Haslam, M. Linka, J. Napier, H.E. Neuhaus, A.P.M. Weber, Peroxisomal ATP import is essential for seedling development in *Arabidopsis thaliana*, Plant Cell 20 (2008) 3241–3257.
[70] M.J. van der Merwe, S. Osorio, W.L. Araújo, I. Balbo, A. Nunes-Nesi, E. Maximova, R. Carrari, V.I. Bunik, S. Persson, A.R. Fernie, Tricarboxylic acid cycle activity regulates tomato root growth via effects on secondary cell wall production, Plant Physiol. 153 (2010) 611–618.
[71] T. Obata, A.R. Fernie, The use of metabolomics to dissect plant responses to abiotic stresses, Cell. Mol. Life Sci. 69 (2012) 3225–3243.